Tunneling $\alpha^2F(\omega)$ and heat-capacity measurements in high-T_c Nb_3Ge

K. E. Kihlstrom
Code 6634 Naval Research Laboratories, Washington, D.C. 20375

D. Mael
Department of Applied Physics, Stanford University, Stanford, California 94305

T. H. Geballe
Department of Applied Physics, Stanford University, Stanford, California 94305
and AT&T Bell Laboratories, Murray Hill, New Jersey 07974

(Received 15 August 1983)

Improved film synthesis has allowed us to prepare $Nb_3Ge/SiO_x/Pb$ tunnel junctions on samples with high T_c (up to 21.2 K) and large energy gap (Δ_{Nb_3Ge} up to 3.85 meV). These junctions have satisfactory features for taking derivative measurements. The data were reduced by the modified McMillan-Rowell proximity gap inversion analysis developed by Arnold and Wolf to generate $\alpha^2F(\omega)$ and related microscopic parameters. The trend previously seen of a movement of the lowest phonon branch to lower energies as the T_c and gap increase is continued, resulting in the lowest-energy phonon mode being well defined and enhanced in strength. Theoretical functional derivatives for T_c (by Bergmann and Rainer) and the energy gap (by Mitrovic *et al.*) qualitatively explain the rise in T_c, energy gap, and $2\Delta/k_BT_c$. Heat-capacity measurements have been performed on various samples to give bulk Nb_3Ge properties, including one sample which was analyzed by tunneling $\alpha^2F(\omega)$ and heat capacity. $\gamma=34\pm1.5$ mJ/mole K^2 and the bare density of states, $N(0)=1.5\pm0.1$ states/eV atom, suggests that a high density of states is inadequate to explain the high T_c in Nb_3Ge. Values for $2\Delta/k_BT_c=4.2\pm0.1$ and $\Delta C/\gamma T_c\sim1.9$ indicate a strong-coupled superconductor, in agreement with tunneling results on this sample.

INTRODUCTION

The high-T_c $A15$ compounds are of continuing interest both for their technological applications as well as for information they can provide into a fundamental understanding of superconductivity. As the material with the highest known T_c,[1] Nb_3Ge is particularly interesting. The most direct probe of microscopic superconductivity is tunneling. Kihlstrom and Geballe[2] produced tunneling $\alpha^2F(\omega)$ on NbGe samples with a wide range of compositions (17–23 at. % Ge), gaps ($\Delta_{Nb_3Ge}\sim1.1$–3.7 meV), and T_c's (7–20 K). The one limitation of the study was the difficulty in producing good quality high-T_c samples. Since that time we have had greater success in producing more homogeneous, high-T_c Nb_3Ge samples.[3] The high T_c has allowed us to extend the tunneling study to make meaningful comparisons with bulk properties via heat-capacity measurements.

TUNNELING

The Nb_3Ge thin films were prepared by electron-beam codeposition[4] in the presence of oxygen.[5,6] The substrate temperature was 900 °C; the deposition rate was ~30 Å/sec. The oxygen partial pressure was 1.3×10^{-6} Torr. The film samples while still under vacuum were cooled to 100 °C and the barrier of 25–30 Å of Si (Ref. 7) was deposited. The samples were then removed from vacuum, and the amorphous Si was allowed to oxidize in air for 24–48 h before the junction area was defined by a dielectric (photoresist). A Pb counterelectrode was then deposited.

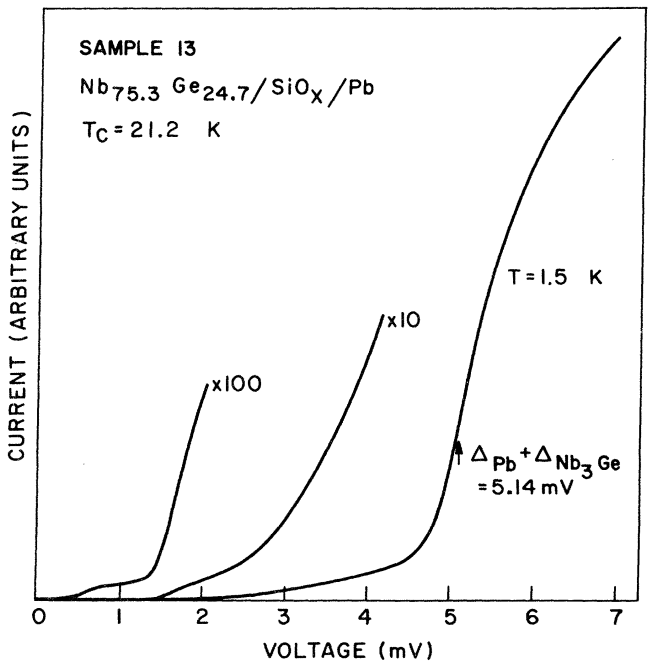

FIG. 1. Current-voltage characteristics for the largest-gap sample in this study.

TABLE I. Physical properties of the samples used in this $\alpha^2F(\omega)$ study.

Sample	Ge (at. %)	$\Delta_{Nb\text{-}Ge}+\Delta_{Pb}$ (meV)	T_c (K)
8	24.3	4.83	20.1
9	24.7	4.90	20.3
10	25.7	4.99	20.2
11	25.7	5.01	19.8
12	24.7	5.14	21.2
13	24.7	5.17	21.2

The current-voltage characteristics for the largest-gap sample in this study are shown in Fig. 1. The Nb_3Ge energy gap for this sample is $\Delta_{Nb_3Ge}=3.85$ meV with a T_c of 21.2 K. There is more excess conductance below the sum gap than for those samples of our previous study[2] (as well as the other samples of this study). Excess conductance is treated as a parallel conductance which does not contribute to the superconducting properties. This is normalized out as done by Schmidt *et al.*[8] Physical properties of these samples are given in Table I. Unlike our previous study, T_c is not determined by gap opening (i.e., the highest temperature at which structure in the derivative of the I-V curve at zero bias is observed). These data were taken, but it was later discovered that the calibration of the carbon thermometer had drifted.[9] Therefore T_c was taken as the midpoint of the transition measured inductively; in the past this has correlated reasonably well with the gap opening T_c. The inductive T_c widths range from 0.4—0.8 K, and any differences with gap opening T_c should not be significant.

The ratio $2\Delta/k_BT_c$, a measure of coupling strength, is plotted in Fig. 2. The gap is determined as the voltage at the minimum of the derivative (dV/dI) through the gap (after subtracting off the Pb gap). Samples with Ge-poor compositions (<21 at. % Ge) show weak-coupled BCS-like values near 3.5, but samples which are nearer stoichiometry show values increasing to 4.3, indicative of strong coupling.

The differential conductance for these samples was measured in the superconducting state with the Pb electrode driven normal by an applied magnetic field of 0.1 T, and then with the temperature elevated above T_c so that both electrodes were normal. The reduced tunneling density of states was then entered into the McMillan-Rowell inversion program[10] to obtain the Eliashberg function $\alpha^2F(\omega)$. To obtain more sensible results we found it necessary to resort to the modified McMillan-Rowell (MMR) gap-inversion analysis developed by Arnold and Wolf.[11–13] The proximity parameters used were comparable to those used previously.

Figure 3 shows the $\alpha^2F(\omega)$ results from the small-gap sample, a mid-range—gap sample (both from the previous study[2]), and two large-gap samples from this study. The smaller of the two new samples fits in well with previous results. The larger-gap sample shows continued enhancement in the lowest-energy phonon branch, now clearly resolved from the other two peaks, as well as additional

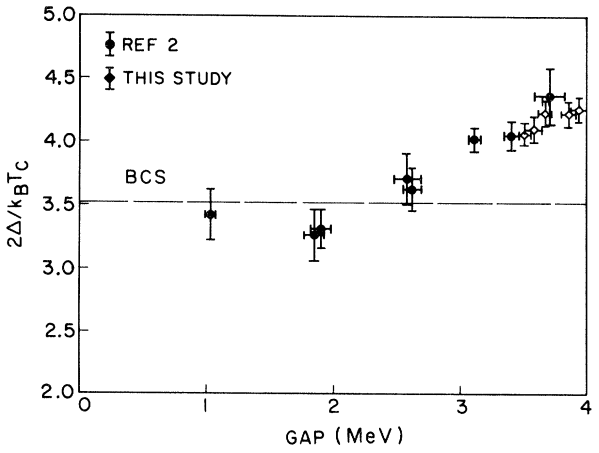

FIG. 2. Variation with gap of the coupling constant $2\Delta/k_BT_c$ for Nb-Ge samples over a wide range of composition. Vertical error bars represent both the finite T_c width (10—90 % of the transition width of the samples in this study) and the uncertainty in estimating the gap.

movement to lower energies. Figure 4 shows the two larger-gap samples (of Fig. 3) compared with $\alpha^2F(\omega)$ from the largest-gap sample, whose I-V trace is shown in Fig. 1. The lowest-energy peak indeed is still stronger in intensity in the largest-gap sample, but the peak position has been shifted back towards higher energies. In fact, all of the peaks show a movement to higher energies (in contrast to the other samples in the study where only the low-energy peak showed movement from sample to sample) as if the x axis were artificially expanded. Second-derivative measurement data (taken separately from the first-derivative data used to generate density of states) confirm the peak positions. We have no clear explanation for the behavior of this sample other than the fact that the sample has passed the stability limit due to mode softening. The metastable phase boundary has been exceeded as judged by the increased excess conductance below the sum gap in the I-V curve shown in Fig. 1 (even though there was no

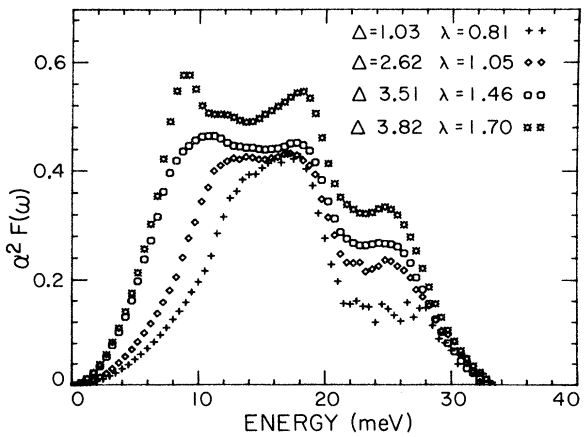

FIG. 3. Electron-phonon spectral function $\alpha^2F(\omega)$ for four Nb-Ge samples with gaps of 1.03, 2.62, 3.50, and 3.82 meV, respectively.

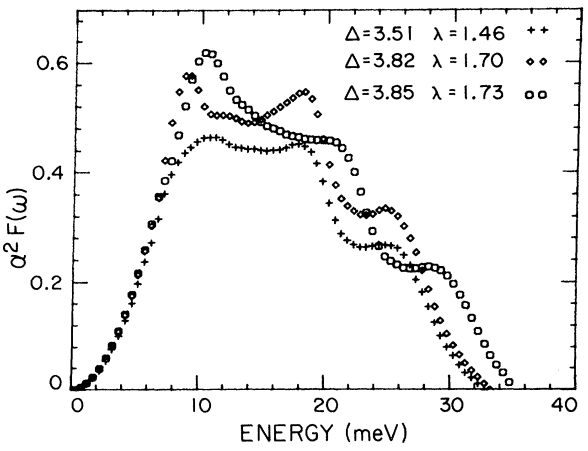

FIG. 4. Electron-phonon spectral function $\alpha^2F(\omega)$ for three high-T_c Nb-Ge samples.

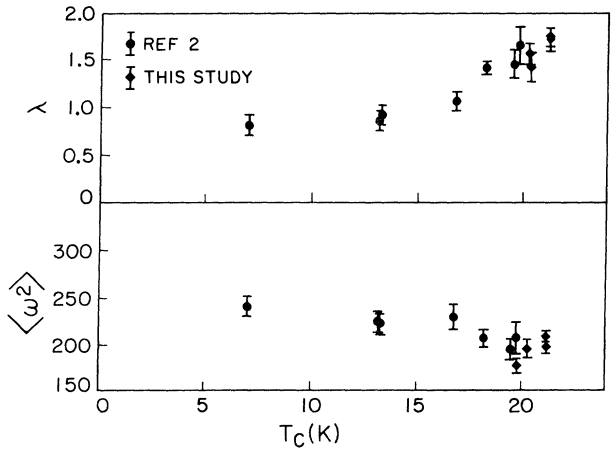

FIG. 5. λ and $\langle\omega^2\rangle$ plotted vs T_c for Nb-Ge samples over a wide range in composition.

second phase evident in the x-ray diffraction data). Values of λ and $\langle\omega^2\rangle$ vs T_c for all the samples in both studies are plotted in Fig. 5. There is a clear trend of higher λ with higher T_c reaching a value of 1.73 ± 0.10 in the highest-T_c sample while $\langle\omega^2\rangle$ shows a decreasing trend.

CALCULATIONS FOR T_c and $2\Delta/k_BT_c$

Geilikman and Kresin[14] gave an analytical formula for $2\Delta/k_BT_c$,

$$2\Delta/k_BT_c=3.53[1+5.3(k_BT_c/\omega_0)^2\ln(\omega_0/k_BT_c)] .$$

Thus an increase T_c relative to ω_0 would increase $2\Delta/k_BT_c$. With the microscopic parameters now available we can test the formula for $2\Delta/k_BT_c$ from Geilikman and Kresin (GK). Now, it is not clear what frequency should be used, but Mitrovic *et al.*[15] suggest both

$$\langle\omega\rangle=(2/\lambda)\int d\omega\,\alpha^2F(\omega)$$

and

$$\omega_{\log}=(2/\lambda)\int d\omega\,\omega^{-1}(\ln\omega)\alpha^2F(\omega)$$

are good choices. Figure 6 shows a comparison between the measured $2\Delta/k_BT_c$ and the calculated values using both $\langle\omega\rangle$ and $\omega_{\log}$. The agreement is better using $\langle\omega\rangle$, although both fail in the off-stoichiometry samples. In the strong-coupled region the agreement is reasonably good.

There have been several attempts to calculate T_c from microscopic parameters using the Eliashberg theory. McMillan[16] solved the finite-temperature Eliashberg equations to find T_c for various cases and constructed an approximate T_c equation:

$$T_c=\frac{\Theta_D}{1.45}\exp\left[-\frac{1.04(1+\lambda)}{\lambda-\mu^*(1+0.62\lambda)}\right] .$$

Dynes[17] replaced the prefactor $\Theta_D/1.45$ (where Θ_D is the Debye temperature) by $\langle\omega\rangle/1.20$. The electron-phonon coupling constant is given by

$$\lambda=2\int_0^\infty d\omega\frac{\alpha^2F(\omega)}{\omega} , \quad \langle\omega^n\rangle=\frac{2}{\lambda}\int d\omega\,\omega^{n-1}\alpha^2F(\omega) .$$

Allen and Dynes[18] found a more accurate numerical solution for T_c than the McMillan equation for materials with $\lambda>1.5$:

$$T_c=\frac{f_1f_2\omega_{\log}}{1.2}\exp\left[-\frac{1.04(1+\lambda)}{\lambda-\mu^*(1+0.62\lambda)}\right] .$$

f_1 and f_2 each go to 1 in the weak-coupling (small-λ) limit. For large λ, f_1 (the strong-coupling correction) varies as $\lambda^{1/2}$ while f_2 (the shape correction) varies as $\langle\omega^2\rangle^{1/2}/\omega_{\log}$. In Fig. 7 we compare the measured T_c's with the calculated T_c's using both methods. In general, the McMillan equation gives slightly better agreement.

In the same paper,[18] Allen and Dynes set up a method to calculate T_c by solving the linearized Eliashberg equations in matrix form using $\alpha^2F(\omega)$ and μ^*. We have used a computer program written in our laboratory by S. Bending, using the $\alpha^2F(\omega)$ and μ^* values determined by tunneling to calculate the T_c's shown in Fig. 8. The agreement (typically 10—15%) is about the same as that obtained using either the McMillan or the Allen and Dynes equations. Since all three methods are derived from the

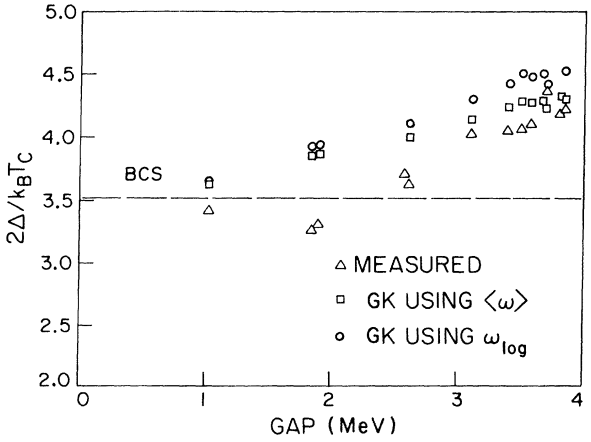

FIG. 6. Coupling strength $(2\Delta/k_BT_c)$ vs gap comparing experimental values with the Geilikman-Kresin (GK) calculated values using $\langle\omega\rangle$ and $\omega_{\log}$.

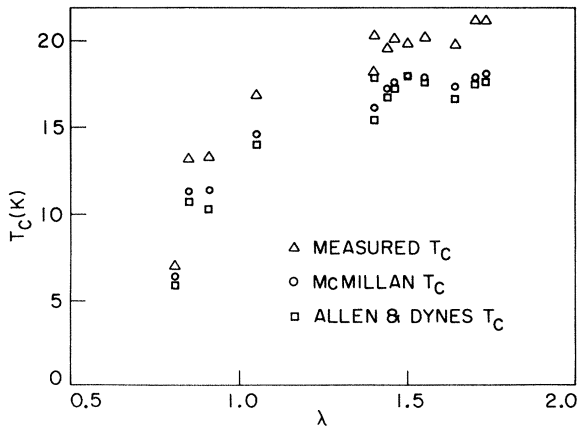

FIG. 7. T_c vs λ comparing experimental T_c values with calculated values by the McMillan and the Allen and Dynes equations.

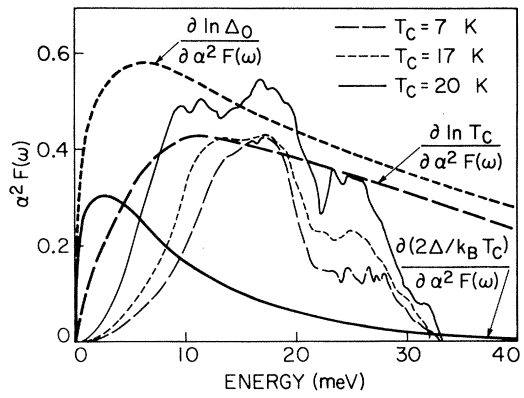

FIG. 9. Theoretical functional derivatives overlaid on the electron-phonon spectral function $\alpha^2F(\omega)$ for three samples. As T_c increases, the low-energy phonon peak moves toward the peaks in the functional derivatives.

Eliashberg equations, this agreement suggests that the approximations made in the McMillan and the Allen and Dynes equations are relatively good for this system. The tunneling results along with the $2\Delta/k_BT_c$ and T_c results from the first study[2] and this study are shown in Tables II(a) and II(b), respectively.

The question of how variations in $\alpha^2F(\omega)$ affect T_c and the energy gap Δ have been addressed by Bergmann and Rainer[19] and by Mitrovic *et al.*[20] They calculated the functional derivatives $\delta T_c/\delta\alpha^2F(\omega)$ and $\delta\Delta/\delta\alpha^2F(\omega)$, respectively. Bergmann and Rainer found that

$$\Delta T_c = \int_0^\infty d\omega \frac{\delta T_c}{\delta\alpha^2F(\omega)} \Delta\alpha^2F(\omega)$$

starts linearly at the origin, has a maximum at $\omega \sim 8k_BT_c$, then decreases (but remains positive) at higher frequencies.

Mitrovic *et al.* calculated the functional derivatives for Δ_0 and $2\Delta/k_BT_c$ for several materials (including Nb_3Sn) and found a relatively universal shape. However, the peak for the gap comes at a lower frequency $\sim 4k_BT_c$, causing the functional derivative for $2\Delta/k_BT_c$ to be peaked at an even lower frequency, $1.3k_BT_c$.

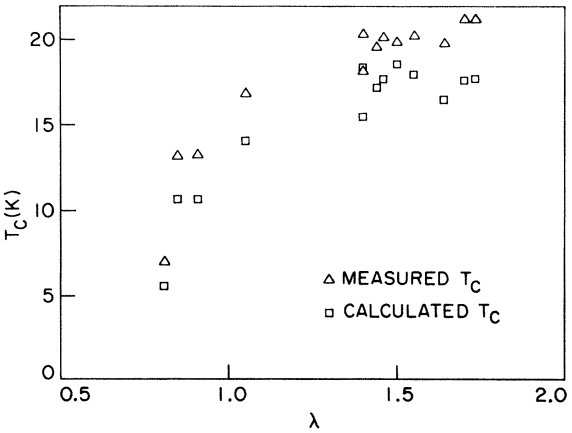

FIG. 8. T_c vs λ comparing experimental T_c values with calculated values by the linearized Eliashberg equations using the full $\alpha^2F(\omega)$.

Figure 9 shows the functional derivatives (calculated for Nb_3Sn, which should be similar to Nb_3Ge) overlaid on three $\alpha^2F(\omega)$ curves. Note, first of all, that the movement of the lowest-energy phonon branch takes that branch toward the peak of the functional derivative for T_c. Thus T_c should increase maximally as $\alpha^2F(\omega)$ is increased. The fact that $\alpha^2F(\omega)$ is also increasing at higher frequencies is less important because the functional derivative for T_c is less there (in contrast to the effect of lessening the decrease in the frequency moments—a disadvantage from the point of view of the T_c equations of Allen and Dynes and of McMillan). Second, the movement of the phonon peak toward the peak in $2\Delta/k_BT_c$ is consistent with the observed increase in $2\Delta/k_BT_c$. Thus there is qualitative agreement between the data on Nb_3Ge and the treatments of Bergmann and Rainer and Mitrovic *et al.*

CALORIMETRIC DATA

Heat-capacity measurements characterize the entire sample. However, until recently the investigations have required considerably larger samples than the thin films used in tunneling. Techniques developed in our laboratory by Early *et al.*[20] have now made it possible to do tunnel-

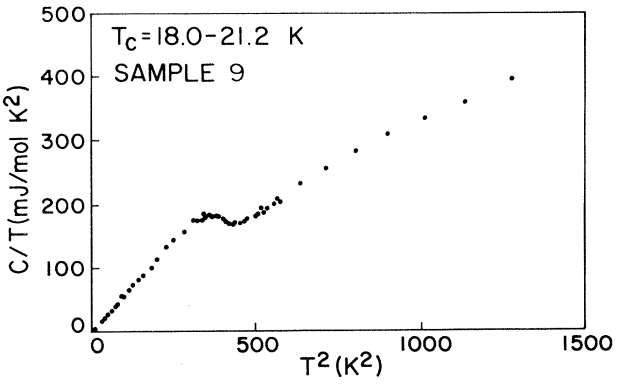

FIG. 10. Plot of C/T vs T^2 for Nb_3Ge (sample 9).

TABLE II. (a) Parameters of samples used in first (Ref. 2) $\alpha^2F(\omega)$ study. (b) Parameters used in this study. Note: The ± values shown for λ, μ^*, and the frequency moments represent variations in the range of the proximity values shown. This range allowed reasonable agreement between the experimental and calculated values for both the tunneling density of states and the cutoff frequency.

	(a) Samples used in Ref. 2						
	1	2	3	4	5	6	7
Parameters							
Composition (at. % Ge)	16.7	21.3	21.3	21.8	22.3	22.8	23.9
$\Delta_{Nb\text{-}Ge}$ (meV)	1.03	1.85	1.90	2.62	3.11	3.40	3.70
T_c (gap opening)	7.0	13.2	13.3	16.8	18.2	19.5	19.8
$2\Delta/k_BT_c$	3.4 ±0.2	3.3 ±0.15	3.25±0.2	3.6 ±0.17	4.0 ±0.1	4.05±0.11	4.35±0.2
Low-energy fit (meV)	10	8.75	8.75	7.75	6	5.25	5
Proximity parameters							
R (10^{-4})	0 ±15	10 ±15	10 ±15	55 ±25	50 ±15	50 ±15	70 ±15
d/L (10^{-3})	0 ±30	20 ±20	20 ±20	80 ±15	70 ±5	70 ±10	70 ±15
λ	0.81±0.11	0.85±0.1	0.91±0.1	1.05±0.12	1.40±0.07	1.44±0.15	1.64±0.2
μ^*	0.13±0.07	0.05±0.04	0.06±0.04	0.05±0.05	0.09±0.03	0.07±0.05	0.12±0.04
$\langle\omega\rangle$ (±0.2) (meV)	14.3	13.7	13.7	13.8	12.7	12.4	12.7
ω_{log} (±0.2) (meV)	12.74	12.2	12.1	12.1	10.8	10.5	10.6
$\langle\omega^2\rangle$ (10) (meV^2)	241	224	222	229	206	195	207
T_c (K) McMillan	6.4	11.3	11.4	14.6	16.1	17.2	17.3
T_c (K) Allen and Dynes	5.9	10.7	10.3	14.0	15.4	16.7	16.6
T_c (K) $\alpha^2F(\omega)$	5.6	10.7	10.6	14.1	15.4	17.15	16.5
$2\Delta/k_BT_c$ GK, ω_0	3.64	3.85	3.86	3.99	4.13	4.22	4.21
$2\Delta/k_BT_c$ GK, ω_{log}	3.66	3.92	3.93	4.10	4.29	4.41	4.41

TABLE II. (*Continued.*)

	(b) Samples used in this study					
	8	9	10	11	12	13
Parameters						
Composition (at. % Ge)	24.3	24.7	25.7	25.7	24.7	24.7
$\Delta_{Nb\text{-}Ge}$ (meV)	3.51	3.58	3.67	3.69	3.82	3.85
T_c (midpoint inductive)	20.1	20.3[a]	20.1	19.8	21.2	21.2
$2\Delta/k_BT_c$	4.05±0.1	4.1 ±0.1	4.2 ±0.1	4.3 ±0.1	4.2 ±0.1	4.2 ±0.1
Low-energy fit (meV)	5.25	5.5	4.5	4.75	5.75	6.25
Proximity parameters						
R (10^{-4})	60 ±10	65 ±15	75 ±10	60 ±10	90 ±10	0 ±10
d/L (10^{-3})	60 ±10	65 ±15	75 ±10	60 ±10	90 ±10	0 ±10
λ	1.46±0.1	1.40±0.15	1.55±0.11	1.50±0.1	1.70±0.12	1.73±0.1
μ^*	0.06±0.03	0.04±0.035	0.07±0.03	0.05±0.03	0.11±0.04	0.12±0.03
$\langle\omega\rangle$ (±0.1)(meV)	12.1	12.4	12.1	11.7	12.4	12.6
ω_{log} (±0.1)(meV)	10.2	10.5	10.25	9.9	10.4	10.6
$\langle\omega^2\rangle$ (±8)(meV^2)	189	195	188	176	196	208
T_c (K) McMillan	17.6	18.05	17.85	18.0	17.85	18.1
T_c (K) Allen and Dynes	17.2	17.8	17.6	17.9	17.45	17.6
T_c (K) $\alpha^2F(\omega)$	17.6	18.3	17.9	18.5	17.6	17.7
$2\Delta/k_BT_c$ GK, ω_0	4.27	4.26	4.28	4.27	4.31	4.29
$2\Delta/k_BT_c$ GK, ω_{log}	4.49	4.46	4.49	4.50	4.53	4.51

[a]Gap opening T_c.

ing and heat-capacity measurements on the same films—containing as little as 100 μg of the sample. The material is evaporated onto the sapphire side of a silicon-on-sapphire wafer (dimensions $6\times6\times0.2$ mm^3). The silicon side had been previously patterned into a resistance thermometer and resistance heater. The wafer is then mounted onto a temperature-controlled copper block by 0.001-in. Au—7 wt. % Cu wires, which provide known thermal and electrical conductivities. The heat capacity is then measured by heating the sample to a known temperature above the block, then measuring the temperature relaxation as heat is conducted away through the wires when the heater is turned off. The relaxation time constant (τ) gives the heat capacity (C) since $\tau = C/K$, where K is the thermal conductance of the wires.

Figure 10 shows the C/T-vs-T^2 curve for a sample on which we also have data from superconducting tunneling. In an ideal sample there would be a discontinuous jump in the specific heat at the transition temperature, but in any real material the rise is spread out over a finite ΔT. For metastable compounds such as Nb_3Ge this is especially true. The transition width for this sample is 3.2 K, which is comparable to the best previous results on Nb_3Ge by Stewart *et al.*[21] The lack of separate jumps as well as the fact that C/T goes to zero as $T\to0$ indicates there is no low-T_c phase or residual normal material (unless it is a small amount spread over a large temperature range).

Other material properties can be obtained from the data by modeling the normal-state specific heat as $C_v=\gamma T+\beta T^3$ and plotting the data as C_v/T vs T^2. The extrapolation to $T^2=0$ gives γ (the coefficient of the normal electronic specific heat), and the slope above T_c^2 gives β (the coefficient of the lattice specific heat). These numbers can be determined to within $\sim5\%$, using the constraint upon the entropy imposed by the third law. From these parameters we then obtain the electronic density of states at the Fermi level where

$$N^*(0)=\left[\frac{2\pi^2k_B^2}{3}\right]^{-1}\gamma$$

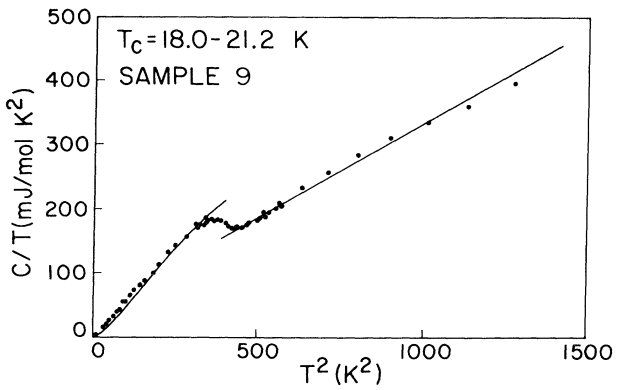

FIG. 11. Plot of C/T vs T^2 for Nb_3Ge comparing experimental values with the calculated fits to the data.

and Θ_D, the Debye temperature ($\beta=1944r/\Theta_D^3$, where $r=4$, the number of atoms per Nb_3Ge molecule). The bare density of states can then be obtained using the value of λ obtained from tunneling as $N(0)=N^*(0)/(1+\lambda)$.

The results are $\gamma=34\pm3$ mJ/mol K^2, which gives $N^*(0)=3.7\pm0.2$ states/eV atom. Using the tunneling value of $\lambda=1.4$ we obtain bare density of states $N(0)=1.5\pm0.1$ states/eV atom. $\beta=0.296\pm0.01$ mJ/mol K^4 (which gives $\Theta_D=297\pm3$ K).

In addition to the above-mentioned normal-state properties, two superconducting properties come out of heat-capacity measurements. The first is $\Delta C/\gamma T_c$. In our material the transition is narrow enough to estimate ΔC by extrapolation of C_s to T_c. This procedure gives a value $\Delta C/\gamma T_c=1.9$, appreciably higher than the BCS value of 1.43, again an indication of strong coupling. The other superconducting parameter, still another measure of coupling strength, is $2\Delta/k_BT_c$. This is obtained by fitting the superconducting electronic specific heat $[C_{\rm els}=C(T)_{\rm tot}-\beta T^3]$ below T_c to the low-temperature approximation $C_{\rm el}\propto\exp(-\Delta/k_BT)$. The fit must be made sufficiently below T_c so that the gap has roughly leveled off to its $T=0$ value. For this sample we obtain the value $2\Delta/k_BT_c=4.1\pm0.1$, which again is consistent

TABLE III. Superconducting parameters from heat-capacity measurements.

Parameter	9	B	Nb_3Ge[a]	Nb_3Al[b]	Nb_3Sn[c]	V_3Si[d]
T_c (K)	21.0	20.0	21.8	18.7	17.9	17.0
γ (mJ/mole K^2)	34 ±3	28.0±2	30.3	36	35	62.8
Θ_D (K)	297 ±3	313 ±3	302	283	270 ($T>T_c$) 204($T=0$)	435($T>T_c$) 297($T=0$)
$2\Delta/k_BT_c$	4.2±0.1	4.8±0.1	4.2	5.6		3.77
$\Delta C/\gamma T_c$	1.9±0.05	2.0±0.05	2.3	3.2	3.5	
λ	1.4	1.4	1.7	1.7	1.7	1.3
$N^*(0)$ (states/eV atom)	3.7±0.2	3.0±0.2	3.2	3.8	3.7	5.6
$N(0)$ (states/eV atom)	1.5±0.1	1.2±0.2	1.2	1.4	1.4	2.4
$N(0)$ theory[e] (states/eV atom)	1.2	1.2	1.2	1.8	1.5	2.4

[a]Stewart *et al.* (Ref. 21).
[b]Cort *et al.* (Ref. 23).
[c]Stewart *et al.* (Ref. 24)
[d]Junod and Muller (Ref. 25).
[e]Klein *et al.* (Ref. 29).

with the tunneling results. Figure 11 shows an overlay of the C/T-vs-T^2 data with the various fits to the data that produced the parameters just quoted. The agreement is good except for the low-temperature data, which show excess heat capacity. There is no distinct transition (as with the 3.06-K material that showed up as a second gap in tunneling experiments reported by Rowell *et al.*[22]). However, as already noted, it is possible that there is a small amount of low-T_c material with a very broad T_c.

As noted earlier, sample 9 has also been analyzed by tunneling (see Table II), T_c, and x ray ($a_0=5.141$ Å) measurements. Table III gives the parameters derived from the heat-capacity measurements in comparison to results from Nb_3Al (Cort *et al.*[23]), Nb_3Sn (Stewart *et al.*[24]), V_3Si (Junod and Muller[25]), and Nb_3Ge (Stewart *et al.*[21]). Also included are the results for a second Nb_3Ge sample (B) from which we did not extract tunneling information and which has a T_c roughly a degree lower than comparable transition widths. Values for λ, needed to calculate $N(0)$, the bare density of states, are obtained from the tunneling studies of Kwo and Geballe[26] for Nb_3Al, Rudman and Beasley[27] for Nb_3Sn, and this work for Nb_3Ge and the infrared study of McKnight *et al.*[28] for V_3Si. The theoretical calculations for the bare density of states is from Klein *et al.*[29]

$2\Delta/k_BT_c=4.8$ for sample B, as measured by heat capacity, is substantially higher than that typically found in tunneling experiments. Also for B the value of γ is lower than the higher-T_c sample 9. It would be interesting to determine how γ, N^*, (0), and $N(0)$ vary with T_c in NbGe. This will require either heat-capacity or critical-field measurements on NbGe with a range of compositions (these experiments are planned).

SUMMARY

Analysis of $\alpha^2F(\omega)$ spectra shows a sharpening of the lowest-energy phonon branch and a shift to lower energies as the composition of Ge is increased beyond its equilibrium value. The composition-spread study allows us to observe an increase in λ and a decreasing trend in $\langle\omega^2\rangle$ as T_c increases. Mode softening plays an important role in high-T_c material as has been previously demonstrated in Nb_3Al (Ref. 26) and in Nb_3Sn (Ref. 27). Common behavior such as the cutoff in $2\Delta/kT_c$ at ~ 4.5 is obtained at the limit of the Ge-, Al-, or Sn-rich side of the phase boundary. (This limit has evidently been just exceeded by the highest-T_c sample, Figs. 1 and 3.) This commonality is consistent with the suggestion that the softening of the mode which connects the $A15$ structure with the neighboring Sn-, Al-, or Ge-rich phase (the so-called Hyde rotation in the case of Al and Ge) defines the metastable limit.[30] We have used the microscopic parameters generated to test several relationships for T_c and $2\Delta/k_BT_c$. We found there was fairly good agreement between the measurements and calculations for T_c by using the empirical McMillan and Allen and Dynes equations. Using the full $\alpha^2F(\omega)$ and solving the linearized Eliashberg equations give agreement comparable to that provided by the empirical equations. The Geilikman-Kresin equation for $2\Delta/k_BT_c$ agrees poorly in niobium-rich material, but as stoichiometry is approached agreement improves. Improved agreement was obtained using $\langle\omega\rangle$ rather than $\omega_{\log}$. The quantitative results are given in Table II. Note that while parameters such as λ and $\langle\omega\rangle^2$ are relatively insensitive to the choice of proximity parameters, μ^* is very sensitive. For instance, a variation in the choice of the parameters that causes λ to vary by 10% would cause μ^* to vary by over 30%.

The functional derivatives of Bergmann and Rainer[19] for T_c and Mitrovic *et al.*[15] for Δ and $2\Delta/k_BT_c$ give qualitative agreement with the observed trends relating mode softening in $\alpha^2F(\omega)$ to those quantities. It would be interesting to make the comparisons quantitatively. Anderson *et al.*[31] have suggested that the degradation of T_c with increasing resistivity in many high-T_c systems is due to increasing Coulomb repulsion (and thus an increase in μ^*). Our tunneling results do not show any systematic indication of this (see Table II), but again μ^* is not very well determined when the proximity analysis is used. Thus a role of μ^* in degradation of T_c in off-stoichiometric NbGe cannot be ruled out. Recently, Rowell *et al.*[32] demonstrated that the use of artificial aluminum oxide barriers on sputtered niobium eliminated the need for the proximity analysis where it previously had been needed. We made a preliminary attempt to extend this to our electron-beam codeposited Nb_3Ge without success.

By combining tunneling $\alpha^2F(\omega)$ with heat-capacity measurements we have been able to obtain a wide variety of superconducting parameters. That the heat-capacity measurements show agreement with the results of tunneling gives evidence that both measurements are producing valid results in the attempt to understand the basic mechanisms of superconductivity in Nb_3Ge. The moderate value of the density of states (1.5 ± 0.1 states/eV atom) compared to that of Nb (2 states/eV atom) and V_3Si (2.4 states/eV atom) suggests that attributing the high-transition temperature in Nb_3Ge to a peak in the density of states at the Fermi surface is not a valid hypothesis. Mode softening is at least partially responsible for the high-T_c superconductivity in Nb_3Ge.

In this work we have tried to apply state-of-the-art theory to state-of-the-art experiments on the highest-temperature superconductor. The results are satisfactory from a semiquantitative point of view, but improvements in synthesis and/or theory are still needed before a fully quantitative understanding of the $A15$ superconductors is achieved.

Two experiments are suggested by this work. One (as mentioned already) is to look at γ, $N^*(0)$, and $N(0)$ as a function of composition in NbGe. The other is to look at tunneling $\alpha^2F(\omega)$ as a function of composition in a high density-of-states $A15$ superconductor (e.g., V_3Si) where mode softening might not be needed to produce the high T_c.

ACKNOWLEDGMENTS

We would like to thank R. H. Hammond and D. A. Rudman for valuable discussions and experimental assistance. This work was supported by the Air Force Office of Scientific Research Contract No. F49620-78-C-0009.

[1]J. R. Gavaler, Appl. Phys. Lett. 23, 480 (1973); L. R. Testardi, R. L. Meek, J. M. Poate, W. A. Royer, A. R. Storm, and J. H. Wernick, Phys. Rev. B 11, 4304 (1975).

[2]K. E. Kihlstrom and T. H. Geballe, Phys. Rev. B 24, 4101 (1981).

[3]K. E. Kihlstrom, R. H. Hammond, J. Talvacchio, T. H. Geballe, A. K. Green, and Victor Rehn, J. App. Phys. 53, 8907 (1982).

[4]For details on the electron-beam evaporator see R. H. Hammond, IEEE Trans. Magn. MAG-11, 201 (1975); J. Vac. Sci. Technol. 15, 382 (1978).

[5]R. A. Sigsbee, Appl. Phys. Lett. 29, 211 (1976); IEEE Trans. Magn. MAG-13, 307 (1977).

[6]A. B. Hallak, R. H. Hammond, and T. H. Geballe, Appl. Phys. Lett. 29, 314 (1976); A. B. Hallak, R. H. Hammond, T. H. Geballe, and R. B. Zubeck, IEEE Trans. Magn. MAG-13, 311 (1977).

[7]D. A. Rudman and M. R. Beasley, Appl. Phys. Lett. 36, 1010 (1980).

[8]P. H. Schmidt, E. G. Spencer, D. C. Joy, and J. M. Rowell, in *Superconductivity in d- and f-Band Metals,* edited by D. H. Douglass (Plenum, New York, 1976), p. 431.

[9]After the discovery of the temperature-scale error, samples from the earlier study were remeasured for gap-opening T_c using a different probe with calibrated thermometry. In all cases the T_c's agreed with the earlier measurements indicating that the temperature-scale drift occurred after the earlier study was completed. Damage on cycling prevented a similar remeasurement on most of the samples from this study.

[10]W. L. McMillan and J. M. Rowell, in *Superconductivity,* edited by R. D. Parks (Decker, New York, 1969), Vol. 1, p. 561.

[11]G. B. Arnold, Phys. Rev. B 18, 1076 (1978).

[12]E. L. Wolf, J. Zasadzinski, J. W. Osmun, and G. B. Arnold, Solid State Commun. 31, 321 (1979).

[13]E. L. Wolf, J. Zasadzinski, G. B. Arnold, D. F. Moore, J. M. Rowell, and M. R. Beasley, Phys. Rev. B 22, 1214 (1980).

[14]B. T. Geilikman and V. Z. Kresin, Fiz. Tverd. Tela (Leningrad) 7, 3294 (1965) [Sov. Phys.—Solid State 7, 2659 (1966)]; Phys. Lett. 40A, 123 (1972).

[15]B. Mitrovic, C. R. Leavens, and J. P. Carbotte, Phys. Rev. B 21, 5048 (1980).

[16]W. L. McMillan, Phys. Rev. 167, 331 (1968).

[17]R. C. Dynes, Solid State Commun. 10, 615 (1972).

[18]P. B. Allen and R. C. Dynes, Phys. Rev. B 12, 905 (1975).

[19]G. Bergmann and D. Rainer, Z. Phys. 263, 59 (1973).

[20]S. R. Early, F. Hellman, J. Marshall, and T. H. Geballe, Physica 107B, 327 (1981).

[21]G. R. Stewart, L. R. Newkirk, and F. A. Valencia, Solid State Commun. 26, 417 (1978).

[22]J. M. Rowell, P. H. Schmidt, E. G. Spencer, P. D. Dernier, and D. C. Joy, IEEE Trans. Magn. 13, 644 (1977).

[23]B. Cort, G. R. Stewart, C. L. Snead, Jr., A. R. Sweedler, and S. Moehlecke, Phys. Rev. B 24, 3794 (1981).

[24]G. R. Stewart, B. Cort, and G. W. Webb, Phys. Rev. B 24, 3841 (1981).

[25]A. Junod and J. Muller, Solid State Commun. 36, 721 (1980).

[26]J. Kwo and T. H. Geballe, Phys. Rev. B 23, 3230 (1981).

[27]D. A. Rudman and M. R. Beasley, Bull. Am. Phys. Soc. 26, 211, (1981).

[28]S. W. McKnight, B. L. Bean, and S. Perkowitz, Phys. Rev. B 19, 1437 (1979).

[29]B. M. Klein, L. L. Boyer, D. A. Papaconstantopoulos, and L. F. Mattheiss, Phys. Rev. B 18, 6411 (1978).

[30]T. H. Geballe, R. H. Hammond, and J. Kwo, in *Synthesis and Properties of Metastable Phases,* edited by E. S. Machlin and T. H. Rowland (American Institute of Mechanical Engineers, New York, 1980).

[31]P. W. Anderson, K. A. Muttalib, and T. V. Ramakrishnan, Phys. Rev. B 28, 117 (1983); K. A. Muttalib, *ibid.* 27, 4628 (1983).

[32]J. M. Rowell, M. Gurvitch, and J. Geerk, Phys. Rev. B 24, 2278 (1981).